Phase behaviour of colloids in confining geometry

2001 J. Phys.: Condens. Matter 13 R321

(http://iopscience.iop.org/0953-8984/13/20/201)

INSTITUTE OF PHYSICS PUBLISHING JOURNAL OF PHYSICS: CONDENSED MATTER

J. Phys.: Condens. Matter **13** (2001) R321–R336 www.iop.org/Journals/cm PII: S0953-8984(01)06118-5

TOPICAL REVIEW

Phase behaviour of colloids in confining geometry

Clemens Bechinger[1] **and Erwin Frey**[2]

[1] Department of Physics, University of Konstanz, 78457 Germany
[2] Department of Physics, Harvard University, Cambridge, MA 02138, USA

Received 15 January 2001

Abstract

We review recent experimental and theoretical studies on two-dimensional (2D) melting in the presence of a one-dimensional (1D) periodic potential. It is demonstrated that a colloidal suspension which is exposed to the interference pattern of two overlapping laser beams show a phase behaviour being totally different from that of 2D systems on homogeneous substrates. This is attributed to the role of particle fluctuations which in the presence of sufficiently strong periodic external potentials enhance particle interactions and thus promote crystallization.

1. Introduction

The physics of melting and freezing of two-dimensional (2D) systems is rather different from their counterparts in three dimensions (3D). While the change from the solid to the liquid phase in 3D is characterized by a first order transition, almost 30 years ago it was suggested that the character of the melting transitions in 2D is fundamentally different. According to the ideas of Kosterlitz–Thouless–Halperin–Nelson–Young (KTHNY) 2D solids melt via two sequential continuous phase transition [1–4]. The first transition is from the solid with quasi-long-range positional order and long-range bond orientational order to a phase with short-range positional order and quasi-long-range bond orientational order, the so-called hexatic phase. This transition is driven by the dissociation of topological defects, i.e. bound dislocation pairs in the solid. The second transition transforms the hexatic phase to a liquid phase in which both positional and orientational order have short ranges. This transition is caused by the dissociation of individual dislocations to form disclinations.

Besides its theoretical interest on the physics of 2D melting the underlying physics is also relevant from the experimental point of view as can be seen by the increasing demand on 2D systems within the rapid technological development of the last decades. Examples are the quantum-Hall effect which is observed in 2D semiconducting devices, or 2D magnetic materials which offer superior properties for future magnetic memory devices. While most of the theoretical work on 2D melting, however, considered only the interactions within 2D objects, real 2D systems do not exist as self-containing objects but are typically confined to solid or liquid substrates. Accordingly, their properties are closely related to the interactions with the underlying substrate. In the case of a crystal, the substrate atoms provide a laterally modulated potential for a 2D adsorbate system. It has been shown theoretically, that this

0953-8984/01/200321+16$30.00

situation leads to a—compared to homogeneous substrates—very different phase behaviour which is due to the interplay of interactions between the adsorbate particles among themselves and with the under laying periodic substrate [5]. While some of these aspects have been already investigated on an atomic scale—with krypton films on graphite probably being the most thoroughly studied system (for a review see e.g. [6])—systematic measurements with atomic systems turn out to be rather difficult since the shape and form of the substrate potential can be only varied within narrow limits.

In the context of fundamental studies of 2D melting, colloidal suspensions, i.e. Brownian particles which are suspended in a liquid, have been proven to be convenient model systems which provide ideal conditions for experimental and theoretical studies [7–10]. Since the pair interaction potential of colloidal particles can be varied over a large range, this allows their interaction to be changed from essentially hard sphere behaviour to e.g. a long-range dipole-dipole interaction. Accordingly, such systems have been intensively investigated as model systems for 2D melting during the last decades and confirmed the 2D melting scenario as described above [8, 10]. While there exist numerous studies on 2D melting on homogenous substrates, only little is known about 2D melting on surfaces with periodic potentials, although the latter is more relevant to the situation experienced by an atomic adsorbate on a crystalline surface. In this paper we summarize some of our recent experimental and theoretical work on the behaviour of colloidal particles in the presence of external potentials. Here we will address the simple case of an one-dimensional (1D) periodic potential which is shown to alter the phase behaviour of the 2D colloidal suspension significantly.

2. Experimental studies

In our experiments we used aqueous suspensions of polystyrene spheres with 3μm diameter and a polydispersity of 4% (Interfacial Dynamics Corp.), which are confined between two horizontally aligned parallel glass surfaces with a spacing of 20 μm. Due to sulfate-terminated surface groups which partially dissociate off when in contact with water, the suspended particles are negatively charged and experience a partially screened electrostatic repulsion which can be described by [11, 12]

$$\Phi(r) = \frac{(Z^*e)^2}{4\pi\varepsilon\varepsilon_0}\left(\frac{\exp(\kappa R)}{1+\kappa R}\right)^2 \frac{\exp(-\kappa r)}{r}. \tag{1}$$

Here Z^*e is the renormalized charge of the particles which has been roughly determined to be $Z^* \approx 20000$ [13], ε is the dielectric constant of water, κ is the inverse Debye screening length and r is the distance between particle centres. The experiments are performed in highly-deionized water using a closed circuit, in which the suspension is pumped through a vessel of ion exchange resin [14]. From the measurement of the ionic conductivity, the Debye screening length is estimated to be on the order of 400 nm.

A convenient way to create spatially modulated potentials for colloidal suspensions has been suggested by Chowdhury and coworkers who demonstrated that a 2D layer of colloidal spheres can be influenced by an optical interference pattern. Since the depth and periodicity of such a light potential can be easily controlled *in situ* (in contrast to e.g. photolithographically formed substrate potentials), this method allows the systematic investigation of the influence of substrate potentials on the phase behaviour of 2D systems.

In order to generate 1D periodic potentials as they will be used in the present study, we first divided the beam of a frequency-doubled Nd:YVO_4 laser ($\lambda = 532$ nm, $P_{max} = 2$ W) into two beams of equal intensity and directed them from above in a slightly-tilted manner into the sample where an interference pattern is produced (figure 1). Since the PS particles

are polarized in the presence of the light field, the interference pattern leads to a periodic, 1D potential $V(x)$ which acts on the particles [15]

$$V(x) = -V_0(1 + \cos(2\pi x/d)). \tag{2}$$

Here $V_0 = (6n_W^2 P\sigma_0^3(n^2-1)/(n^2+2)cr_0^2)[j_1(\pi\sigma_0/d)d/2\pi\sigma_0]$ is the amplitude of the potential with P being the laser power, c the velocity of light in vacuum, n the ratio of the refractive indices of polystyrene n_P and water n_W, σ_0 the colloidal particle diameter, j_1 the first-order spherical Bessel function, r_0 the waist radius of the gaussian laser beam, and d the line spacing of the interference pattern. The validity of equation (2) has been experimentally confirmed by using highly diluted colloidal suspensions. From their equilibrium distribution function the light potential has been found to agree with the above formula within 10% [16]. Since in addition to equation (2) the intensity profile shows a gaussian envelope, we used only the central region of the interference pattern for the data evaluation to guarantee V_0 to be constant within about 5% . Because the two laser beams are directed almost perpendicular onto the sample the particles in addition experience a vertical light pressure which pushes them towards the negatively-charged bottom silica plate of our cell [17]. This vertical force is estimated to be in the range of pN and largely reduces vertical fluctuations of the particles, thus confining the system effectively to two dimensions. In order to keep this light pressure independent of V_0, one of the laser beams was directed through a λ/2-plate to rotate the polarization of one beam with respect to the other. Accordingly, the variation of V_0 could be achieved by adjusting the angle of the λ/2-plate while keeping the total laser intensity constant. The sample was in addition illuminated with white light from the top and imaged with a microscope objective onto a CCD camera chip connected to a computer for further analysis. The intense Nd:YVO_4 laser light was blocked with an optical filter [18].

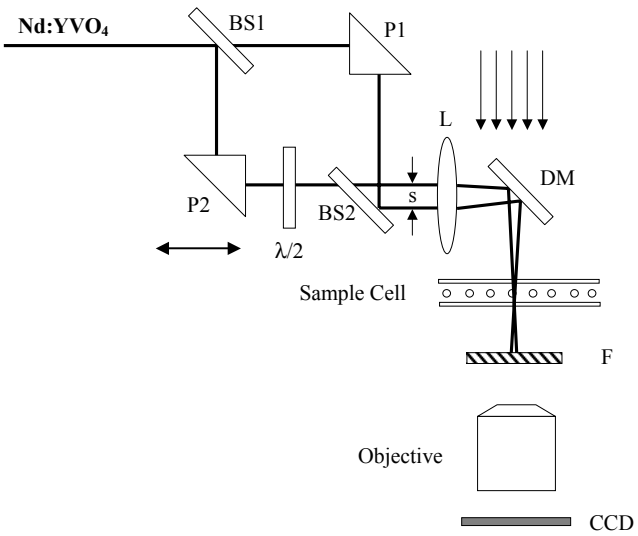

Figure 1. Schematic view of the optical setup. An incident laser beam is first splitted into two beams of equal intensity by means of the beamsplitters (BS1, BS2) and the prisms (P1, P2) and then overlapped inside the sample plane with the lens (L) and a dichroic mirror (DM). The position of P2 can be varied to change the beam spacing s and thus the fringe spacing d of the resulting interference pattern. The amplitude of the intensity modulation is controlled by the position of a λ/2-plate which is inserted in one of the laser beams. The sample is illuminated with white light from above to allow imaging of the particles onto a CCD camera. The camera is protected with a filter to avoid exposure to the high intensity of the incoming laser beam.

In our experiments we have chosen the colloid density to be somewhat below that required for spontaneous crystallization. In the absence of the periodic light potential the particles thus form an isotropic liquid, with mean particle distance a= 9.6 μm (figures 2(a) and (b)). Upon exposing the sample to a weak horizontally aligned interference pattern with $V_0 = 0.6k_BT$ the isotropy of the system is broken and the particles prefer to align in horizontal strings corresponding to the symmetry of the underlying interference fringes (figures 2(c) and (d)). The exponential decay of the pair correlation function along those lines clearly indicates that in this direction this phase is liquid. Since perpendicular to the laser fringes (vertical direction in figure 2.) the particle density is modulated, this phase is termed a *modulated liquid* [19]. When the light potential is increased to $V_0 = 2.1k_BT$ we observe a transition into a crystalline structure with quasi-long-range order (figures 2(e) and (f)). The triangular symmetry is due to the fact that the distance between the interference lines is chosen to be commensurate, i.e. $d = a\cos 30^\circ$; otherwise a distorted lattice is obtained. This remarkable transition which has been reported for the first time by Chowdhury and coworkers in 1985 [20] is readily understood when taking into account that even in the liquid phase the particles prefer to arrange in local hexagons. While for sufficiently small V_0 these hexagons are orientated randomly, with increasing V_0 they become more and more aligned to the light pattern until they form a crystal [21, 15].

What would happen if one increases the potential strength V_0? Obviously this would further reduce particle fluctuations perpendicular to the interference fringes and one might anticipate—in the spirit of the Lindemann criterion (see below)—that the crystalline phase becomes even more pronounced. Experimentally, however, we observe just the opposite. As can be seen in figures 2(g) and (h), which were obtained for $V_0 = 6.3k_BT$, the triangular order disappears and the crystal remelts (light-induced melting, LIM) back into a modulated liquid.

To understand the origin of this effect, it is helpful to realize that even in the crystalline phase the particles perform considerable fluctuations up to 30% around their equilibrium positions (see figure 2(f)). The fluctuations perpendicular to the laser potential, in the presence of the strongly repulsive interparticle interactions, are essential for the registration of neighbouring lines and thus for the occurrence of quasi-long-range order. In that sense, fluctuations *stabilize* the crystalline phase (figure 3(a)). Consequently, when those fluctuations are *reduced* by increasing V_0, the coupling between adjacent lines is weakened, and the crystal *remelts* to a modulated liquid (figure 3(b)). The scenario described here, is strikingly different from that usually observed in 2D systems on homogeneous substrates and emphasizes the importance of the interaction of the particles with the external (light) potential which must—in addition to particle–particle interactions—be taken into account. As demonstrated in the above experiments, it is the counter-play between these two interactions which is responsible for the observed phase behaviour.

To stress this important point in some more detail, in addition to the above measurements, where the particle number density was held constant, we also measured the phase behaviour for different particle number densities as a function of the light potential amplitude V_0. Particular attention was paid to the fact that the periodicity of the laser potential d was adjusted properly to obtain a hexagonal crystal, i.e. $d = \frac{\sqrt{3}}{2}a$, otherwise a distorted lattice is observed. The d-values were varied approximately between 6 μm and 8 μm. The result of more than 100 single measurements are shown in figure 4 in the $(\kappa a)^{-1}$ versus V_0 plane, with a being the mean distance of next-neighbour particles which has been measured for each particle concentration in the absence of the laser field [16]. As can be seen, the value of $(\kappa a)^{-1}$ where the transition towards the crystal occurs decreases at small laser intensities as a function of V_0. This is the characteristic feature of LIF. For larger values of V_0, however, the separation line between the crystalline and the modulated liquid region is shifted back to higher $(\kappa a)^{-1}$-values and starts to

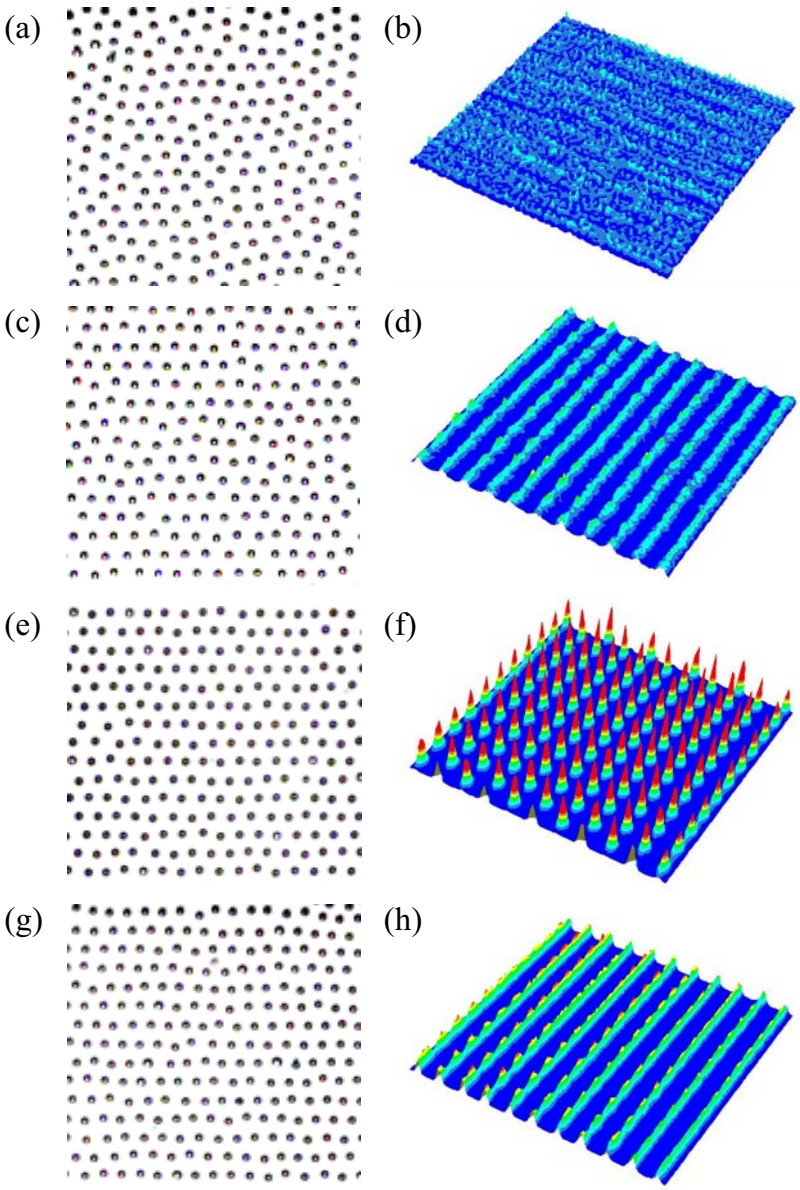

Figure 2. Left column: Typical configurational snapshots of colloidal particles inside a 2D cell, additionally exposed to an optical interference pattern which is aligned horizontally. Right column: from single video pictures the particle centres have been determined by a computer program to calculate the averaged single particle density $\rho(x, y)$ which is plotted here in perspectivic view. To obtain sufficient statistics the data were averaged over 200 pictures, with time delays of 3s each. The data correspond to zero light potential (a,b) and three nonzero potential values $(c, d)0.6k_BT$, $(e, f)2.1k_BT$ and $(g, h)6.3k_BT$.

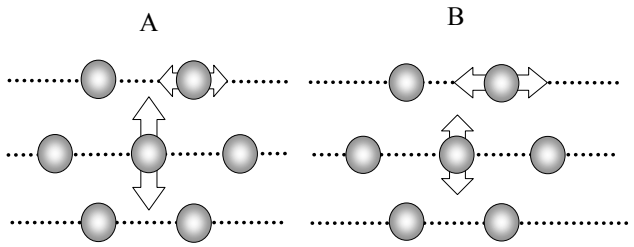

Figure 3. Schematic illustration of how fluctuations affect the particle interaction in neighbouring minima of the laser potential (dashed lines). The vertical and horizontal arrows denote the strength of the particle interactions perpendicular and along the laser potential. (a) In the crystalline phase particle fluctuations perpendicular to the interference pattern contribute to the registration of adjacent lines. (b) At higher light intensities those particle fluctuations are reduced by the laser field and thus lead to a reduced coupling of adjacent lines which then leads to the reentrant modulated liquid phase.

saturate at the highest values which could be obtained in our setup. It is this up bending which gives rise to the LIM phenomenon. Only if $(\kappa a)^{-1}$ is in a relatively small range between 0.045 and 0.048, with increasing V_0 one observes the following sequence of states: isotropic liquid–modulated liquid–crystal–modulated liquid and supports the sequence observed in figure 2. In addition our data clearly show, that reentrant melting from the crystalline state to a modulated liquid is only observed if the crystalline state had been formed by LIF and underlines the unique properties of the light-induced crystalline state.

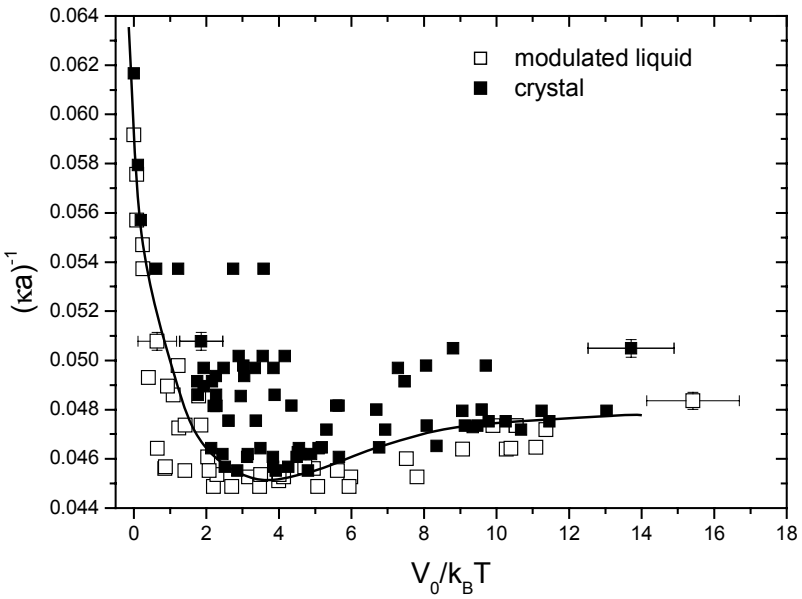

Figure 4. Experimentally determined phase diagram as a function of $(\kappa a)^{-1}$ against V_0/kT. The open symbols denote the modulated liquid and the closed symbols the crystalline phase, respectively. For clarity error bars are only plotted for a few data points. The solid line is a guide to the eye.

3. Theoretical results

There are several reasons why phase transitions in two-dimensional systems are interesting from a theoretical point of view. As the dimensionality of space is reduced, the fluctuations around mean-field behaviour become more pronounced. These fluctuations act to disorder the system and therefore to lower the critical temperature. Eventually they may drive it to zero. These observations are summarized in the Hohenberg–Mermin–Wagner theorem stating that there is no long-range order in a two-dimensional systems with a continuous symmetry group. But, order does not seem to be destroyed altogether. There is still a low-temperature phase with quasi-long-range order, characterized by a power law decay of the order parameter correlation function. This phase is distinct from a high temperature phase with short-range order where correlation functions decay exponentially at large distances. A remarkable result of condensed matter theory is that the excitations driving the transition are not long-wavelength fluctuations in the phase of the order parameter but *topological defects* [1, 22, 23]. Building on these ideas a defect mediated melting theory for 2D melting has been formulated [1–4] with the remarkable result that melting proceeds via a successive unbinding of dislocations and disclinations with a hexatic phase intervening between the solid and liquid phase [2, 3]. In the following we will review how this 2D melting theory is modified by the presence of a 1D periodic potential.

3.1. Order parameters and Landau's mean-field theory

We start our discussion with a mean-field analysis. Despite the fact that mean-field theories are unreliable in low-dimensional systems it is still instructive to review its predictions for two-dimensional melting in the presence of a periodic potential. The basic idea of Landau's mean-field theory is to write down an expansion of the free energy in terms of the order parameters of the system under consideration. In a 2D solid order is characterized by a translational order parameter, $\rho_{\vec{G}}(\vec{r}) = \mathrm{e}^{\mathrm{i}\vec{G}\cdot\vec{r}}$, and an orientational order parameter, $\psi_6(\vec{r}) = \mathrm{e}^{6\mathrm{i}\theta(\vec{r})}$, where $\vec{G}$ is a reciprocal lattice vector, $\vec{r}$ is the position of a colloidal particle, and $\theta(\vec{r})$ is the 'bond' angle between two colloidal particles relative to some reference axis. We chose a geometry where $\vec{G}_1$ is commensurate with the laser potential. Then the form of the coarse-grained free energy functional in terms of the order parameter fields is dictated by symmetry [24, 20]

$$\begin{aligned} F = {} & -2V_0\rho_{\vec{G}_1} + \frac{1}{2}r_T\sum_{\vec{G}}\left|\rho_{\vec{G}}\right|^2 + w_T\sum_{\vec{G}_1+\vec{G}_2+\vec{G}_3=0}\rho_{\vec{G}_1}\rho_{\vec{G}_2}\rho_{\vec{G}_3} \\ & + u_T\left(\sum_{\vec{G}}\left|\rho_{\vec{G}}\right|^2\right)^2 + u_T'\sum_{\vec{G}}\left|\rho_{\vec{G}}\right|^4 + \cdots + \frac{1}{2}r_6|\psi_6|^2 + u_6|\psi_6|^4 + \cdots \\ & + \gamma\sum_{\vec{G}}\left|\rho_{\vec{G}}\right|^2\Big[\psi_6\left(G_x - iG_y\right)^6 + \psi_6^*\left(G_x + iG_y\right)^6\Big]. \end{aligned} \tag{3}$$

The summations run over all wave vectors $\vec{G}_i$ lying on the ring of reciprocal lattice vectors closest to the origin. At high temperature both parameters r_T and r_6 are positive and will eventually change sign when temperature is lowered. In the absence of a laser potential there are two possible scenarios. If r_T changes sign while r_6 is still positive, then because of the cubic term one expects a first-order liquid–solid transition [25]. On the other hand, if r_6 changes sign before r_T mean-field theory predicts a continuous transition into an orientationally ordered hexatic phase with a subsequent hexatic to solid transition. One of the most important effects of the laser potential is that (due to the linear coupling between the amplitude of the laser potential V_0 and the Fourier density mode) a finite value for $\langle\rho_{\vec{G}_1}\rangle$ is induced at all temperatures, even

in the liquid phase. This has two important consequences. First, it leads to an effective field conjugate to the bond orientational order through the coupling γ in equation (3). Second, it converts Landau's cubic term into a simple upward shift in the melting temperature for the only remaining critical mode $\Psi = \rho_{\vec{G}_2} - \rho_{\vec{G}_3}$. Then the resulting Landau expansion contains only even powers of this complex order parameter Ψ, which therefore generically orders via a continuous transition in the XY universality class. Hence, within the mean-field analysis of Chowdhury *et al* [20], one expects to reach a tricritical point upon increasing the laser potential, beyond which the melting transition becomes continuous. These results have been confirmed by density functional theory [26]. Unfortunately, the applicability of mean-field-like theories to problems with continuous symmetry in 2D is limited since these theories drastically underestimate the effect of fluctuations. These fluctuations can suppress the transition temperature so far below its mean-field value that order parameter amplitude fluctuations except in the form of topological defects play no role. In this case a two-stage melting process mediated by the unbinding of dislocations [1–4, 24, 25] and disclinations [2, 3, 25] provides an alternative scenario which we will discuss next.

3.2. Dislocation unbinding theory

3.2.1. Review of 2D melting on a smooth substrate Before discussing the effect of a periodic potential on melting in 2D colloidal systems let us briefly summarize the key results for 2D melting on a smooth substrate. At sufficiently long scales and to quadratic order in the elastic strain

$$u_{ij} = \frac{1}{2}\left(\partial_i u_j + \partial_j u_i\right) \tag{4}$$

associated with the colloidal displacement field $\vec{u}(x, y)$, a 2D hexagonal crystal is well described by isotropic continuum elastic theory

$$F = \frac{1}{2}\int \mathrm{d}^2 r \left(2\mu u_{ij}^2 + \lambda u_{kk}^2\right). \tag{5}$$

The Lame coefficients μ and λ, with μ the usual shear modulus, are the only two elastic constants necessary to completely characterize the elastic energy associated with small deformations of an unperturbed 2D hexagonal solid. As observed by Landau and Peierls in the 1930's thermal excitation of long wavelength phonon modes destroy long-range translational order and lead to a logarithmic divergence in the correlation function of the displacement field. As a consequence there is only quasi-long-range translational order characterized by a power law decay in the correlation function for the translational order parameter

$$\left\langle \rho_{\vec{G}}(\vec{r})\rho_{\vec{G}}(\vec{0})\right\rangle \sim r^{-\bar{\eta}_G} \tag{6}$$

where the temperature dependent exponent

$$\bar{\eta}_G = k_B T \left|\vec{G}^2\right| \frac{3\mu + \lambda}{4\pi\mu\,(2\mu + \lambda)} \tag{7}$$

is inversely related to the stiffness constants of the phonon modes. Unlike the mean square displacement, the expectation value of $\langle\theta^2\rangle$ remains finite [27] and consequently there is long-range bond orientational order at low temperatures.

There are two different types of (topological) defects associated with the continuum elastic theory of a solid: dislocations and disclinations. Dislocations can be generated by removing a half-row of colloids from an otherwise perfect lattice (see figure 5). They are quite effective in destroying translational order but are less disruptive of orientational correlations. The topological "charge" characterizing a dislocation is its Burgers vector $\vec{b}$, defined as the

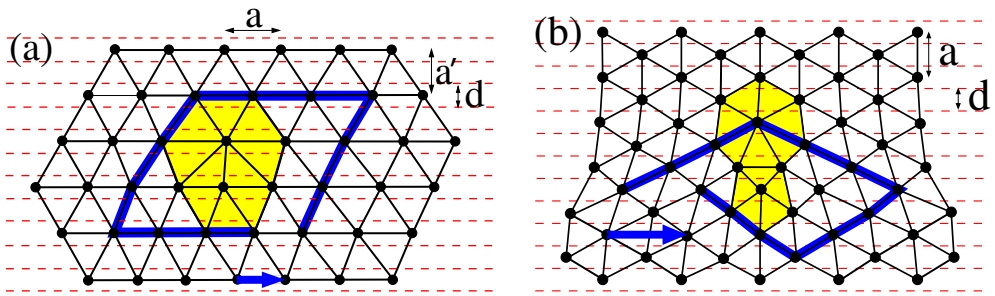

Figure 5. Triangular lattice with lattice constant a subject to a periodic potential (maxima indicated by dashed lines) for two different relative orientations: (A) $p_A d = a'_A$ with $a'_A = \sqrt{3}a/2$ and $p_A = 2$, and (B) $p_B d = a'_B$ with $a'_B = a/2$ and $p_B = 1$. Also shown are low energy dislocations with Burgers vector $\vec{b}$ parallel to the corrugation of the potential.

amount of a closed contour integral of the displacement field around a dislocation fails to close $\oint \mathrm{d}\vec{u} = \vec{b}$. One of the most remarkable results of 2D melting theory is that unbinding of dislocation pairs drives a transition from a solid not directly to a liquid but to a *hexatic phase* [3], where translational order is short-range but there is still quasi-long-range orientational order. A transition from the hexatic to a liquid phase occurs only at a higher temperature where dissociation of disclination pairs destroys orientational correlations.

3.2.2. Induced hexatic order Since many potential applications of 2D melting theory are to films adsorbed onto a crystalline substrate, it is important to ask how the melting scenario described above is modified by the effect of commensurate or incommensurate periodic potentials. Because of the 'substrate' tunability the colloidal system described above allows us to address this question in a rather unique way. The most obvious effect of the periodic substrate is that it explicitly breaks continuous 2D rotational symmetry down to rotations by 180°. In other words, the favoured orientations for the 'bonds' between the colloidal particles is parallel to the troughs of the laser potential and the hexatic order parameter is finite at all temperatures. This situation is analogous to a ferromagnet in a magnetic field, where the qualitative distinction between paramagnetic and ferromagnetic phase in erased in an external magnetic field, with both phases displaying a finite induced magnetization. Here, the laser potential eliminates the continuous transition from an isotropic liquid to a hexatic liquid phase. The hexatic order parameter ψ_6 at low laser intensities show power law behaviour

$$\psi_6 \propto V_0^{1/\delta_6} \tag{8}$$

with $1/\delta_6 = 6$ in the liquid phase and

$$1/\delta_6 = \frac{6\eta_6}{4 - \eta_6} \tag{9}$$

in the hexatic phase, where η_6 is the exponent describing the algebraic decay of bond orientational order in the absence of the laser-induced periodic potential.

3.2.3. The locked floating solid The periodic potential also changes the nature of the low temperature phase. While the particles are pinned transversely to the troughs of the periodic potential, executing only massive optical phonon-like excitations in that direction, they are able to slide freely along the potential minima with acoustic phonon excitations within the troughs. Because of these highly anisotropic properties this phase has been called 'locked

floating solid' (LFS) [28]. Upon integrating out the optical phonon-like u_y-modes the LFS can be described in terms of an elastic free energy for the acoustic u_x-modes

$$F_{LFS} = \frac{1}{2}\int \mathrm{d}^2 r \left\{ K_{eff}\,(\partial_x u_x)^2 + \mu_{eff}\left(\partial_y u_x\right)^2 \right\} \tag{10}$$

with effective elastic constants K_{eff} and μ_{eff} for compression and shear, respectively. The structure function of a LFS is quite unusual. It displays a set of delta-function Bragg peaks located at the multiples of the laser potential reciprocal lattice vectors $\vec{K} = (2\pi/d)\vec{e}_y$, which coexist with other spontaneously induced Bragg peak along the y-axis and quasi-Bragg peaks for $G_x \neq 0$. The latter show algebraic singularities in the static structure factor, $S(\vec{q}) \sim |\vec{q} - \vec{G}|^{\eta_G - 2}$ with

$$\eta_G = k_B T G_x^2 \frac{1}{2\pi\sqrt{K_{eff}\mu_{eff}}}. \tag{11}$$

A sketch of the structure factor for two typical relative orientations of the triangular lattice with respect to the periodic laser potential is shown in figure 6.

3.2.4. How does the locked floating solid melt? With increasing temperature the locked floating solid will eventually melt. What is the nature of this melting transition, if not preempted (as it can always be) by a first-order transition? What are the relevant topological defects driving the transition? What is the nature of the phase above the melting transition? The answer to these

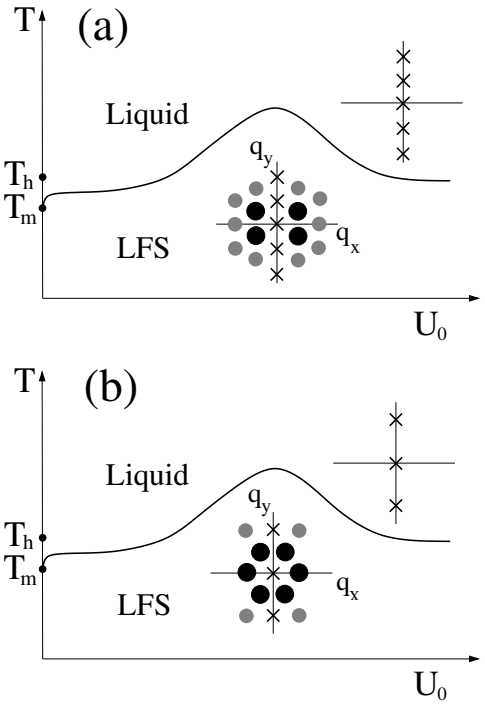

Figure 6. Schematic $p = 1$ phase diagram for orientations A and B. Insets: schematic structure functions in the various phases. The x's indicate delta-function Bragg peaks and circles algebraic peaks. T_h indicates the transition temperature from the hexatic to the liquid phase at zero potential strength.

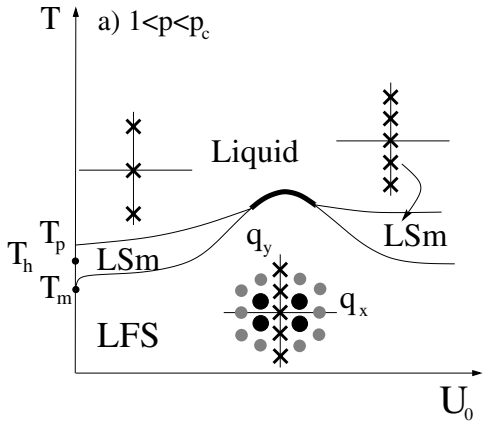

Figure 7. Schematic phase diagram for a primary commensurate orientation with commensurability parameter in the range $1 < p < p_c$ (the case $p = 2$ is shown here). Thin lines indicate continuous phase transitions. The thick line between the LFS and modulated liquid phase is most likely a first-order phase boundary. Insets: schematic structure functions. As in figure 6, the x's indicate delta-function Bragg peaks and the shaded circles algebraic peaks.

questions depends on two important ingredients: (i) the orientation of the triangular colloidal lattice relative to the laser potential, which selects a set of Bragg planes that run parallel to the troughs; and (ii) the commensurability ratio of the spacing a' between these Bragg planes to the period d of the laser potential, defined by $p = a'/d$. In figure 5, two particularly interesting orientations, denoted A and B, of the colloidal crystal and laser potential are shown. A key observation is that only dislocations with a Burgers vector parallel to the troughs have the usual logarithmically divergent energy. In orientation A, four of the six fundamental Burgers vectors are disfavoured by the potential, which would require that they be attached to a semi-infinite discommensuration string. The effect of the periodic potential is even more dramatic in orientation B. Here all six fundamental Burgers vectors are disfavoured. The lowest energy Burgers vector parallel to the laser minima has length $\sqrt{3}a$. Hence (if experimentally feasible) tuning of the relative orientation and the commensurability ratio allows to select the Burgers vector of the dislocations which drive the melting transition. Unlike conventional 2D melting [3], the exponent of the power law Bragg peaks is *universal* at the melting transition, and is given by

$$\eta_G^* = (\vec{G}\vec{b}/4\pi)^2 \tag{12}$$

where $\vec{b}$ is the smallest allowed Burgers vector in the trough direction. For the primary orientation A, illustrated in figure 5(a), with $b = a$, the exponent characterizing the algebraic order in the off-axis peaks (see figure 6(a)) closest to the q_y-axis is $\eta_G^* = 1/4$; for the next row of peaks with $G_x = 4\pi/a$ one finds $\eta_G^* = 1$, consistent with the algebraic decay observed experimentally [19]. For orientation B, with $b = \sqrt{3}a$, the six quasi-Bragg peaks closest to the origin have different power laws; peaks on the x-axis have $\eta_G^* = 1$, whereas the four off-axis peaks have $\eta_G^* = 1/4$.

3.2.5. Topology of the phase diagram The topology of the phase diagram depends on the magnitude of the commensurability parameter p. For $p = 1$, which is the case studied in the experiments described above, the phase diagram contains only two thermodynamically distinct phases. A dislocation unbinding transition in the universality class of the anisotropic

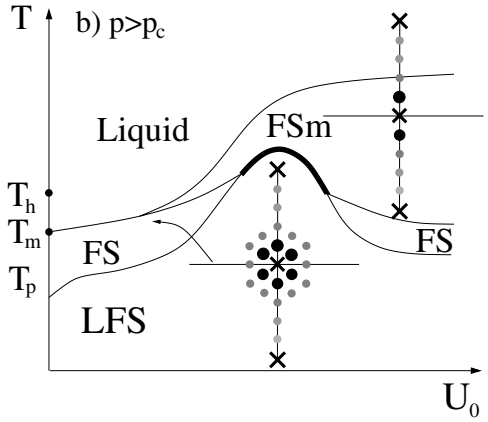

Figure 8. Schematic phase diagram for a primary commensurate orientation with commensurability parameter $p > p_c$ ($p = 4$ is shown here). As in figure 6 the thick line indicates a first-order transition. Insets: schematic structure functions. As in figure 6, the x's indicate delta-function Bragg peaks and the shaded circles algebraic peaks.

XY model melts the LFS to a modulated liquid phase. The most striking feature of this phase transition is the existence of a region in the phase diagram where one finds re-entrant melting. We will discuss below, why such a fascinating re-entrance phenomenon generically emerges in the limit of a short Debye screening length. With increasing commensurability ratio additional intermediate phases between the LFS and modulated liquid become possible. For $1 < p < p_c$, where p_c depends on the relative orientation between the triangular solid and the periodic potential, the dislocation unbinding melts the LFS to a locked smectic phase (LSm). In the LSm phase distinguishes itself from the modulated liquid phase by a broken discrete translational symmetry: only one out of p possible troughs is preferentially occupied by the colloidal particles. As illustrated in figure 7, the structure factor of the LSm phase displays spontaneously induced Bragg peaks at multiples of $\vec{K}/p$ in addition to the Bragg peaks at multiples of $\vec{K}$, directly induced by the laser interference fringes. The transition from the LSm to the modulated liquid phase is in the p-state clock model universality class. A direct transition from the LFS to the modulated liquid phase is still possible. Because it requires a simultaneous loss of a continuous and a discrete symmetry it is most likely a first-order transition. Above a critical commensurability ratio p_c the complexity of the phase diagram further increases (figure 8). The key feature is that now the laser potential becomes irrelevant before the LFS melts. One finds a roughening-like phase transition from the LFS to a floating solid (FS). The melting of the FS to a modulated liquid is in the same universality class as 2D melting on a smooth substrate. Similar to the phase transition from the LFS to the LSm, the melting of the FS phase into the floating smectic (FSm) phase is mediated by the unbinding of dislocation pairs with Burgers vectors parallel to the minima of the periodic potential. An additional subtlety results from the presence of the massless spectator phonon modes transverse to the troughs of the laser potential [29]. It will be interesting to explore all of these theoretical predictions using colloidal systems.

3.2.6. Re-entrance The most surprising feature of the phase diagram is re-entrant melting as a function of the potential strength (see figure 6). At small laser intensities the freezing temperature increases as a function of V_0. This is intuitively understood by taking into account a suppression of thermal fluctuations which reduces the entropy of the liquid phase and hence

makes freezing into a lattice less costly. Actually, it turns out that the shape of the phase boundary at small potential strength shows a universal cusp [29]. On the other hand, for large V_0, one finds theoretically that the melting temperature (for short-ranged interaction between the colloidal particles) generically decreases with increasing laser intensity. This can be understood with a heuristic argument as described above, but also more quantitatively [28]. Note that the effective shear modulus μ_{eff} entering the expression for the melting temperature $T_m = \vec{b}^2\sqrt{K_{eff}\mu_{eff}}/8\pi$ is determined by a screened Coulomb interaction $V(r) = V_0 \exp[-\kappa r]$ between colloidal particles in neighbouring troughs. In order to find an effective shear modulus for the u_x-modes, one needs to integrate out the massive u_y-modes corresponding to displacements perpendicular to the troughs of the laser potential. Upon assuming that the dominant effect comes from the shear modulus and simply averaging the potential over the massive u_y degrees of freedom one finds $\mu_{eff} \propto \left\langle \mathrm{e}^{-\kappa|r_{n=1}-r_n|}\right\rangle_{u_y}$, where r_n and r_{n+1} are positions of nearest-neighbour colloidal particles belonging to the n and $n+1$ laser potential troughs. This gives to lowest harmonic order in the fluctuations [29]

$$\mu_{eff}(V_0) \propto \left\langle \mathrm{e}^{-\kappa a-\kappa[u_y(n+1)-u_y(n)]}\right\rangle \propto \mathrm{e}^{-\kappa a}\mathrm{e}^{\kappa^2\left\langle u_y^2\right\rangle} \approx \mu_{eff}(\infty)e^{const.\times k_BT/V_0}. \tag{13}$$

When combined with the expression for the melting temperature, this reduction in the effective shear modulus implies that the melting temperature increases with decreasing potential strength [28]

$$T_m(V_0) = T_m(\infty)\left\{1 + \frac{5((\kappa a)^2-31)}{64\pi^2}\left(1+\frac{13}{3\kappa a}\right)\frac{k_BT_m(\infty)}{V_0}\right\} \tag{14}$$

thus implying re-entrant melting for a band of temperatures as a function of potential strength. Note that theory also predicts that re-entrant melting should be absent below a critical value $\kappa a \approx 5.6$ of the Debye screening length.

3.3. Monte Carlo simulation

Recent Monte-Carlo simulation studies of melting in the presence of a 1D periodic external potential have explored the phase diagram in the parameter space of V_0/k_BT and κa with particle density and temperature fixed [30, 31, 26]. The results seem to be inconclusive: although earlier simulations [30] claimed to have found a tricritical point at intermediate laser intensities and re-entrance, recent studies from the same laboratory refute these results [31]. These difficulties are perhaps unsurprising, given that even much larger scale simulations have, so far, failed to completely resolve the nature of 2D melting, even without a periodic external potential [32]. One might question whether such simulations are in equilibrium with respect to dislocation climb (or even glide).

Dislocation-unbinding melting theory predicts that

$$\left(\kappa_m^\infty - \kappa_m^0\right)a \approx 2\ln\left(1.3\kappa_m^\infty/\kappa_m^0\right) > 0 \tag{15}$$

which in the dilute limit reduces to $\left(\kappa_m^\infty - \kappa_m^0\right)a \approx 0.52$. In particular, we find $\kappa_m^\infty > \kappa_m^0$ in agreement with experiment [16]. Simulations [30] report the opposite result. More recent simulations from the same group [31] seem to refute these earlier results and find in agreement with our theory $\kappa_m^\infty > \kappa_m^0$. Their numerical value for $\left(\kappa_m^\infty - \kappa_m^0\right)a \approx 1.32$ is, however, roughly two times larger than our asymptotic prediction of 0.52. These deviations should, however, not be taken too seriously, since equation (13) neglects finite renormalization of elastic constants by dislocation dipoles and nonlinear elastic effects, our prediction is an estimate, only accurate up to unknown factors of order 1. It should be mentioned that very recent MC simulations from Strepp *et al* [33] obtain a value which is in the same order of magnitude. The corresponding

value of equation (13) taken from our experimental results in figure 4 is considerably larger than that predicted here, but this difference might be due to the finiteness of our system or the fact that in the experiment the periodic, 1D potential has an gaussian envelope due to the beam profiles of the two interfering laser beams. Attempts are in progress to study the effect of the phase behaviour as a function of the system size.

Next we discuss re-entrance in the $V_0/k_BT - \kappa_m a$ phase diagram. There is a critical value for $\kappa a \approx 5.6$ below which $(\kappa a)^{-1}$ is a monotonically decreasing function of the potential strength. If both $\kappa_m^0 a$ and $\kappa_m^\infty a$ are larger than the critical value 5.6, theory predicts re-entrant behaviour. This re-entrant behaviour is consistent with the experimental results described above. It is also similar to what one finds in simulations [30] at small values of the potential strength. However, there are significant differences. First of all, the type of transition is very different. Whereas we discuss a continuous dislocation mediated melting transition, simulations appear to find a first-order transition. Second, as discussed above, the simulations show $\kappa_m^\infty < \kappa_m^0$ which is opposite to what our theory predicts. In more recent simulations [31] κ_m is found to increase monotonically with potential strength with no sign for re-entrance.

It should be mentioned that the phase behaviour discussed in the paper is not restricted to charged stabilized colloidal suspensions but should be also observed for other pair potentials. Very recently, it has been demonstrated by Strepp *et al* that for hard discs in an external periodic 1D potential a very similar phase diagram is observed [34]. Calculations [35] along similar lines as described in [28, 29] show that re-entrance is expected even for a dipolar interaction between the colloidal particles, i.e. a $1/r^3$ pair potential. In general however, one would expect that the re-entrance behaviour becomes less pronounced with increasing range of interaction of the pair potential.

4. Fluctuations and the Lindemann criterion

We have pointed out that under certain conditions particle fluctuations are actually essential for the occurrence of crystalline order and that melting occurs upon reducing those fluctuations. This seems to contradict the phenomenological melting criterion which was suggested from Lindemann in 1910 [36]. According to his idea, a solid melts when the thermally driven fluctuations of atoms become so strong that neighbouring particles collide with each other. Although this view of atomic collisions turned out to be not strictly correct, both experimental and theoretical investigations confirm Lindemann's basic idea and predict melting to occur when the root mean square displacements of the particles exceed about 10% of the lattice constant [37, 38]. This melting criterion was long thought to be inapplicable to 2D systems due to the lack of true long-range-order which leads to a divergence of the mean square displacement of the particles in the thermodynamic limit. With small modifications, however, the Lindemann melting criterion can be applied to 2D systems [39]. Accordingly, the intuitive idea that particle fluctuations destroy positional order and thus lead to melting is well established in physics. Therefore, at first glance it may sound odd that fluctuations in certain systems should enhance positional order, i.e. promote crystallization. Our apparently paradoxical result is caused by the fact that in the presence of the 1D light potential, the system cannot contract perpendicular to the potential lines when the lateral fluctuation amplitude of the particles is decreased. This, however, is different when considering e.g. an atomic adsorbate on a crystalline surface at constant pressure. In this situation, decreasing the fluctuation strength, e.g. by lowering the temperature, would (in case of an e.g. Lennard-Jones-like interaction potential) lead to a thermal contraction of the crystalline substrate and thus to a smaller mean distance a of the adsorbed particles. As a result one would not follow a horizontal path in the phase diagram as we did in figure 4 but rather cross it with a line with a positive slope. Owing to the fact that

re-entrance is only observed in a relatively small range of $(\kappa a)^{-1}$-values, however, would lead to the absence of the re-entrant melting phenomenon.

5. Summary

In summary, our results demonstrate how the 2D-melting scenario proposed by KTHNY is affected by the presence of a periodic, 1D potential. We have shown that, as the light potential is gradually increased, a 2D liquid first crystallizes in predominantly hexagonal order and then melts again to a modulated liquid. We attributed this rather unusual re-entrance behaviour to the fact that lateral particle fluctuations in the present system contribute to the registration of adjacent lines. Accordingly, when those fluctuations are suppressed by increasing the light field, a remelting of the crystal is observed which demonstrates the ambivalent role of particle fluctuations in such systems.

Acknowledgments

We would like to acknowledge helpful discussions with M Brunner, P Leiderer, D Nelson, L Radzihovsky and Q-H Wei. This work was supported by the Deutsche Forschungsgemeinschaft through a Heisenberg fellowship (Fr 850/3-1) (EF) and the Sonderforschungsbereich 563 (EF) and 513 (CB).

References

[1] Kosterlitz J M and Thouless D J 1973 *J. Phys. C: Solid State Phys.* **6** 1181
[2] Halperin B I and Nelson D R 1978 *Phys. Rev. Lett.* **41** 121
[3] Nelson D R and Halperin B I 1979 *Phys. Rev.* B **19** 2457
[4] Young A P 1979 *Phys. Rev.* B **19** 1855
[5] Coppersmith S N, Fisher D S, Halperin B I, Lee P A and Brinkmann W F 1982 *Phys. Rev.* B **25** 349
[6] Prokrovsky V L 1986 *Solitons* (Amsterdam: North Holland) ch 3 pp 71–127
[7] Marcus A H and Rice S A 1996 *Phys. Rev. Lett.* **77** 2577
[8] Marcus A H and Rice S A 1997 *Phys. Rev.* E **55** 637
[9] Murray C A, Sprenger W O and Wenk R A 1990 *Phys. Rev.* B **42** 688
[10] Zahn K, Lenke R and Maret G 1999 *Phys. Rev. Lett.* **82** 2721
[11] Derjaguin B V and Landau L 1941 *Acta Physicochim URSS* **14** 633
[12] Vervey E J W and Overbeek J T G 1948 *Theory of the stability of lyophobic colloids* (Amsterdam: Elsevier)
[13] Alexander S, Chaikin P M, Grant P, Morales G J and Pincus P 1984 *J. Chem. Phys.* **80** 5776
[14] Palberg T, Härtl W, Wittig U, Versmold H, Würth M and Simnacher E 1992 *J. Phys. Chem.* **96** 8180
[15] Loudiyi K and Ackerson B J 1992 *Physica* A **184** 1
[16] Bechinger C, Brunner M and Leiderer P 2001 *Phys. Rev. Lett.* **86** 930
[17] Ashkin A 1970 *Phys. Rev. Lett.* **24** 156
[18] Bechinger C, Wei Q H and Leiderer P 2000 *J. Phys.: Condens. Matter* **12** A425
[19] Q.-H. Wei, Bechinger C, Rudhardt D and Leiderer P 1998 *Phys. Rev. Lett.* **81** 2606
[20] Chowdhury A, Ackerson B J and Clark N A 1985 *Phys. Rev. Lett.* **55** 833
[21] Ackerson B J and Chowdhury A H 1987 *Faraday Discuss. Chem. Soc.* **83** 309
[22] Berezinskii V L 1971 *Sov. Phys. JETP* **32** 493
[23] Berezinskii V L 1972 *Sov. Phys. JETP* **34** 610
[24] Nelson D R 1983 *Phase transtions and critical phenomena* (London: Academic)
[25] Landau L D 1937 *Phys. Z. Sowjetunion* **II** 26
[26] Chakrabarti J, Krishnamurthy H R and Sood A K 1994 *Phys. Rev. Lett.* **73** 2923
[27] Mermin N D 1968 *Phys. Rev.* **176** 250
[28] Frey E, Nelson D R and Radzihovsky L 1999 *Phys. Rev. Lett.* **83** 2977
[29] Radzihovsky L, Frey E and Nelson D R 2001 *Phys. Rev.* E **63** 31503
[30] Chakrabarti J, Krishnamurthy H R, Sood A K and Sengupta S 1995 *Phys. Rev. Lett.* **75** 2232

[31] Das C 1999 *Preprint* cond-mat/9902006
[32] Bagchi K, Anderson H C and Swope W 1996 *Phys. Rev.* E **53** 3794
[33] Strepp W and Nielaba P private communication
[34] Strepp W, Sengupta S and Nielaba P 2000 *Phys. Rev.* E at press
[35] Frey E unpublished results
[36] Lindemann F A 1910 *Phys. Zeits.* **11** 609
[37] Gilvary J J 1956 *Phys. Rev.* **102** 308
[38] Cho S-A 1982 *J. Phys. F: Met. Phys.* **12** 1069
[39] Bedanov V M, Gadiyak G V and Lozovik Y E 1985 *Phys. Lett.* A **190** 289